E. S. Barrekette
R. L. Christensen

On Plane Blazed Gratings

Abstract: The Fraunhofer patterns of blazed gratings are derived on the basis of a scalar theory which includes the non-linear dependence of the obliquity factor and the phase modulation on the spatial frequencies defining the positions of the source and of the observer. The solution based on the usual 'linear communications' theory is compared with one based on the more general non-linear theory; it is shown that the former is meaningful only in the neighborhood of the blaze wavelength. The behavior of blazed gratings is examined in the light of non-linear theory in the region away from the blaze wavelength. It is shown that the envelope function describing the amplitude distribution due to a single groove depends on the single parameter defining half the phase difference between the two edges of a single diffracting facet. It is also shown that certain wavelengths are missing from the zero order and that 'dark' lines exist into which no light of any order is transmitted. A useful maximum for the aspect ratio is derived. The Littrow and spectrograph configurations are examined in some detail.

Introduction

The diffraction grating is a useful, versatile, and mature tool of the optical profession, which has provided probably the most prominent and lucid example of the "wave interpretation" of photo-optical phenomena. Basic experimental and theoretical investigations of diffraction gratings were conducted early in this century by Wood[1–3] and Lord Rayleigh[4]. The former, for example, discovered the well-known anomalies which bear his name, and the latter investigated gratings theoretically and examined the effects of polarization, achieving results in fairly good agreement with observed values.

Numerous authors have discussed the principles of diffraction gratings with varying degrees of rigor. Recently, Madden and Strong[5] presented a theoretical analysis of plane blazed gratings as well as of the aberrations of some concave gratings. It is our purpose, however, to analyze, in a paper of intermediate mathematical precision, the basic phenomena underlying or attending the use of blazed gratings and to explain the reasons for several of the more prominent phenomena observed, giving physical insight into the mathematical results. Specifically, the ramifications of the blaze concept and the diffraction patterns of plane blazed gratings are examined. The accuracy of the usual linearizations of the communications theory approach is easily tested in the case of gratings and is therefore also examined in some detail. Similar techniques have been used recently to describe finite sinusoidal phase gratings.[6]

It is instructive, as a first approximation, to consider a blazed grating as one whose diffracting (i.e., causing wave interference) surfaces are inclined so as to cause specular reflection to occur in that direction wherein occurs the desired maximum of constructive interference. A simple geometrical analysis following that basic approach can extend the usual description of plane gratings[7] to include blaze and give an approximation to actual results. At the other extreme, a quantitatively rigorous analysis of gratings would necessitate a solution of Maxwell's equations with appropriate boundary conditions and would include the effect of polarization on grating efficiency.

Our approach is based on Fraunhofer's approximation to the Kirchhoff diffraction theory and is thus subject to the limitations of this approximation, including the neglect of polarization effects.* In addition, the usual assumptions are made: namely, the effects of shadowing are neglected (so that our results are valid for those angles of incidence or diffraction for which no point of any groove is in the shadow of another groove); the effects of multiple diffractions are neglected; and the source is assumed to be a uniform and long line-source and the grating grooves are assumed to be parallel to this source and long (to permit a one-dimensional treatment, i.e., to

* It should be noted that polarization effects may prove important in some cases.[8–12] A complete treatment of the problem of energy distribution and efficiency in gratings will be found in Ref. 12.

Figure 1 Configuration of source, object, and field domains: (a) reflection grating; (b) transmission grating.

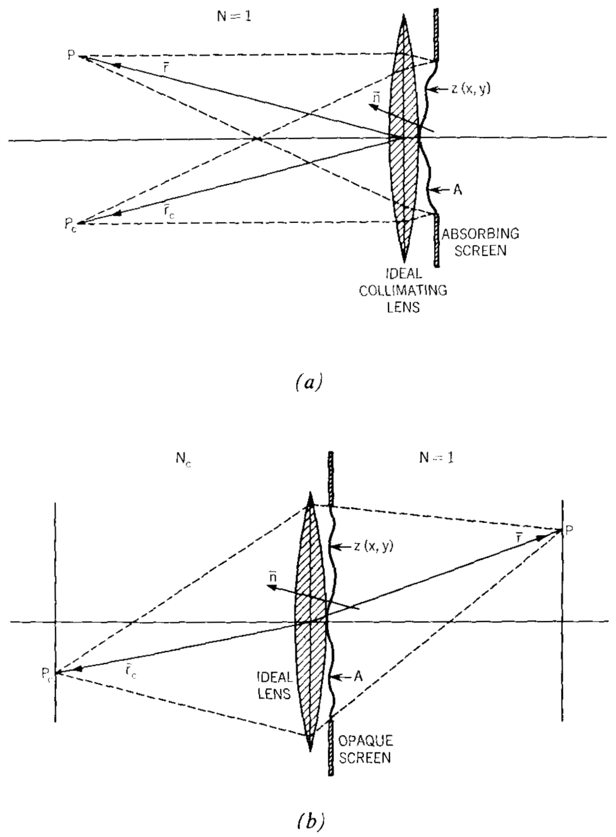

Figure 2 Geometry for the definition of spatial frequency: (a) reflection grating; (b) transmission grating.

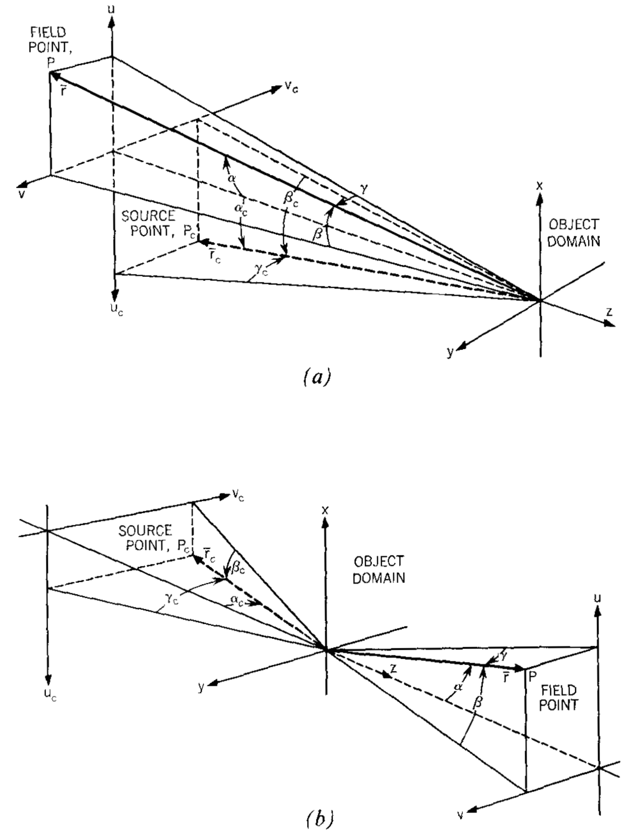

permit variation of light amplitude in the direction of the grooves to be neglected). Finally although the contribution of the minor facets is examined and its affect on the over-all patterns evaluated, it is neglected in most of the results.

Fraunhofer diffraction by blazed gratings

Consider the configuration shown in Fig. 1a. Let P_c be a generic point in the source and let P be a generic point in the Fraunhofer diffraction field. Let the diffracting object be defined by the surface $z(x, y)$ which consists of 1) a region A of uniform unit reflectance, and 2) an absorbing screen everywhere outside of A. The source and field points are in the focal plane of an aberration-free collimating lens whose aperture is greater than the region A. (It should be noted that the following development also applies to a configuration utilizing collimating mirrors).

According to Fraunhofer theory the amplitude distribution $U(P)$ at the field point P due to light of wavelength λ emanating from the source at P_c is given by[5,13]

$$U(P) \approx \qquad (1)$$

$$\cdot \int_A \psi \exp \{i2\pi[\phi z + (\mu_c - \mu)x + (\omega_c - \omega)y]\}\, dA,$$

where integration is carried over the surface $z(x, y)$ within region A; the obliquity factor is $\psi = \frac{1}{2}[\cos(n, r_c) + \cos(n, r)]$; the phase deviation is $2\pi\phi$, where $\phi = (\cos\alpha_c + \cos\alpha)/\lambda$; and $\mu_c = (\sin\beta_c)/\lambda$, $\mu = (\sin\beta)/\lambda$, $\omega_c = (\sin\gamma_c)/\lambda$, $\omega = (\sin\gamma)/\lambda$, are spatial frequencies.[14] The quantities α, α_c, β, β_c, γ, γ_c, r, r_c are geometrical factors defined in Fig. 2a, and n is the outward normal to the diffracting surface.

A transmitting phase-modulating object in the configuration shown in Fig. 1b gives rise to a far-field amplitude distribution which is also described[15] by Relation (1) but for which: $\psi = \frac{1}{2}[N_c\cos(n, r_c) - \cos(n, r)]$; $\phi = (N_c\cos\alpha_c - \cos\alpha)/\lambda$; $\mu_c = (N_c\sin\beta_c)/\lambda$; $\mu = (\sin\beta)/\lambda$; $\omega_c = (N_c\sin\gamma_c)/\lambda$; $\omega = (\sin\gamma)/\lambda$; N_c is the index of refraction of the object; and α, α_c, β, β_c, γ, γ_c, r, r_c, are as defined in Fig. 2b. The object in this case has a unit transmittance in the region A and is opaque elsewhere. (It should be noted that the above result is derived in Ref. 15 subject to the approximation $\psi \approx 1$ and also that for strict rigor, the object, Fig. 1b, should be in collimated light between two lenses such that the source and Fraunhofer field lie in their focal surfaces. The configuration shown approaches the required geometry as the lens approaches an infinite, thin, ideal lens.)

If the source is assumed to be a long line parallel to the y-axis and of uniform intensity, and if the object does not have any variations along this axis, i.e., if $z = z(x)$, then variations of amplitude with y can be neglected. The amplitude distribution is then such that

$$U \approx \int_A \psi \exp \{i2\pi[\phi z + (\nu_c - \nu)x]\} \, ds, \quad (2)$$

where integration is carried with respect to the distance s along that portion of the line of intersection of the grating with the xz plane which falls within the region A, and

$$\nu_c = (\sin \alpha_c)/\lambda; \qquad \nu = (\sin \alpha)/\lambda. \quad (2a)$$

For the case of a transmitting object

$$\nu_c = (N_c \sin \alpha_c)/\lambda. \quad (2b)$$

Let the grating consist of N grooves of blaze angle δ and aspect ratio $e \equiv a/d$ as shown in Fig. 3. Let the narrower facets (for instance, $\overline{BC}$ in Fig. 3) absorb all the light that is incident upon them. Thus, the amplitude distribution can be expressed as

$$U = K\psi \int_{-\infty}^{\infty} o(x) \exp [i2\pi(\nu_c - \nu)x] \, dx, \quad (3)$$

where K is a constant of proportionality which depends on the blaze angle; the intensity of the source; the distances between the source, object, and field domains; and the wavelength of the light emitted by the source. For a grating centered at $x = kd$, and having N grooves each centered at $x = k_n d$ [where, if N is odd, $k_n = k + n$, $n = 0, \pm 1, \pm 2, \cdots \pm \frac{1}{2}(N - 1)$; or, if N is even, $k_n = k + \frac{1}{2} + n$, $n = 0, \pm 1, \cdots \pm(\frac{1}{2}N - 1), -\frac{1}{2}N$], the object function $o(x)$ is such that

$$o(x) = \begin{cases} \exp [i2\pi\phi(x - k_n d) \tan \delta] & \\ \qquad \text{for } |x - k_n d| \leq \frac{1}{2}a; & \\ 0 \qquad \text{for } \frac{1}{2}a \leq |x - k_n d| \leq \frac{1}{2}d; & \\ 0 \qquad \text{for } \frac{1}{2}N < |x - kd|. & \end{cases} \quad (3a)$$

The above expression for $o(x)$ corresponds to the fact that on the *major* facets $|x - k_n d| \leq \frac{1}{2}a$, while on the *minor* facets, $\frac{1}{2}a \leq |x - k_n d| \leq \frac{1}{2}d$. In the regions beyond the ends of the grating we have $\frac{1}{2}N < |x - kd|$. The obliquity factor ψ is, as can be seen from Fig. 3,

$$\psi_r = \tfrac{1}{2}[\cos (\alpha_c + \delta) + \cos (\alpha - \delta)] \quad (3b)$$

(reflecting grating),

$$\psi_t = \tfrac{1}{2}[N_c \cos (\alpha_c + \delta) + \cos (\alpha + \delta)] \quad (3c)$$

(transmitting grating).

In the region $|x - k_n d| \leq \frac{1}{2}a$ where $o(x)$ differs from zero, ψ is independent of x.

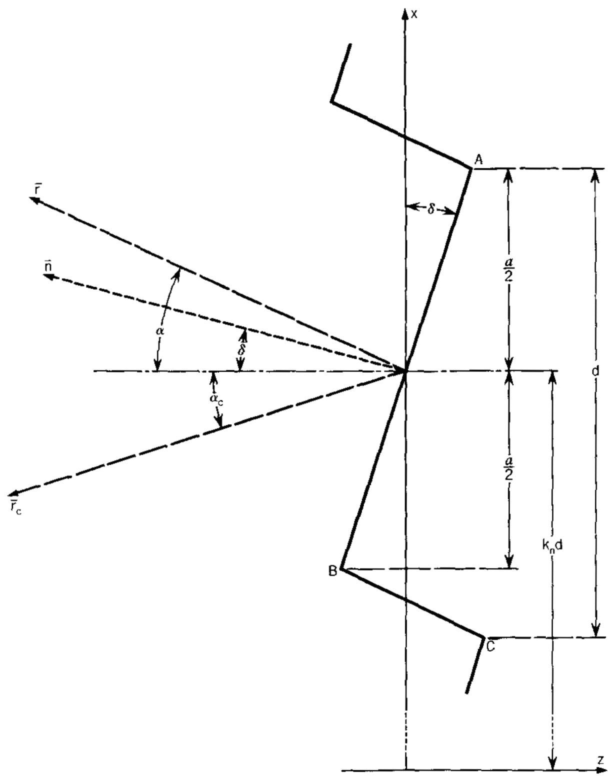

Figure 3 Groove geometry in a blazed grating.

By integrating over a single groove and then summing over the N grooves we obtain

$$U = K\psi I(\nu) E(\nu) \exp [-i2\pi(\nu - \nu_c)kd], \quad (4)$$

where $I(\nu)$, the interference function, is simply the sum of the geometric series

$$\sum_n \exp [-i2\pi(\nu - \nu_c)(k_n - k)d],$$

that is,

$$I(\nu) = \frac{\sin N\pi d(\nu - \nu_c)}{\sin \pi d(\nu - \nu_c)}, \quad (4a)$$

and where $E(\nu)$ is the envelope function describing the amplitude distribution due to a single groove and given by

$$E(\nu) = (a \sin \xi)/\xi, \quad (4b)$$

in which

$$\xi = \pi a[\phi \tan \delta + \nu_c - \nu]. \quad (4c)$$

Spectral content of the zero order

We shall examine the spectral content in the zero order for a reflecting grating in both the spectrograph and the Littrow configurations. The carrier frequency, ν_c, is zero in both configurations when this order is observed.

The zero order occupies that interval for which $|\nu| \leq \nu_0$, where ν_0 is the smallest positive root of $\sin N\pi d\nu = 0$. Thus, in the zero order $|\sin \alpha| \leq \lambda/Nd$ so that for large N we have $\alpha \ll 1$, $\sin \alpha \approx \alpha$. It follows that ψ (provided δ is not too large) and ϕ can be considered constant in this interval; indeed $\psi \approx \cos \delta$ and $\phi \approx 2/\lambda$. In view of Eqs. (4a–c), we have, for $|\alpha| \leq \lambda/Nd$

$$U = \qquad (5)$$

$$Ka \cos \delta \, \frac{\sin(\pi N d\alpha/\lambda) \sin[\pi a(2\tan\delta - \alpha)/\lambda]}{(\pi\, d\alpha/\lambda)[\pi a(2\tan\delta - \alpha)/\lambda]} e^{-i2\pi\alpha k d}$$

We seek the normalized energy distribution as a function of λ, i.e.,

$$\Im(\lambda) = (e\Im_0)^{-1} \int_{-\nu_0}^{\nu_0} U(\nu)\, U^*(\nu)\, d\nu,$$

where integration is carried over α with λ fixed, where U^* is the complex conjugate of U, and where a convenient normalizing factor, $\Im_0$, is the energy that would be reflected into the zero order by a plane mirror of length $Na/\cos \delta$ (equal to the total length of the diffracting facets of the grating) inclined at an angle δ to the optic axis and otherwise placed in the same configuration as the grating.† With some manipulation, we obtain

$$\Im_M(\Lambda) = \qquad (6)$$

$$[2\pi^3 M Si(2\pi)]^{-1} \int_{-M^{-1}}^{M^{-1}} \frac{\sin^2 \pi M\zeta \sin^2[\pi(\zeta\Lambda - 1)/\Lambda]}{[\zeta(\zeta\Lambda - 1)/\Lambda]^2} d\zeta$$

where $M \equiv N/e = Nd/a$ and $\Lambda \equiv \lambda/(2a \tan \delta)$.

As $M \to \infty$ the spectral content of the zero order approaches the form, Fig. 4,

$$\Im_\infty(\Lambda) = [(\Lambda/\pi) \sin(\pi/\Lambda)]^2. \qquad (7)$$

Obviously, $\Im_\infty = 0$ for some values of Λ; *the wavelengths* $\lambda_n = (2a \tan \delta)/n$, $n = 1, 2, \cdots$, *are missing from the zero order*, i.e., $\Im_\infty(\lambda_n) = 0$. Also, $\Im_\infty(\infty) = 1$.

It is interesting to note that $\Im_\infty$ *is a good approximation to* $\Im_M$ *even for relatively short gratings.* For instance, for $M = 100$ (i.e., for a grating with no more than 100 grooves) we find from Eq. (6) that $\Im_{100}(\lambda_n) \leq 1.12 \times 10^{-5}$ while $[1 - \Im_{100}(\infty)] = 4.1 \times 10^{-5}$ so that to all intents *the wave lengths* $\lambda_n = (2a \tan \delta)/n$ *are missing from the zero order of a finite grating.* In effect, then (as has been graphically illustrated by Longhurst[16]) and despite the fact that the width of the principal maxima is inversely proportional to the number of grooves, *the normalized power contained in the principal maxima is relatively insensitive to the number of grooves.* Consequently, in the following sections we shall concern ourselves only with the limiting case $N \to \infty$; our results will then apply to most gratings since generally a grating has so many grooves that its diffraction pattern is very closely approximated by that of a corresponding infinite grating.

† The Fraunhofer diffraction for such a mirror can be obtained from Eq. (3) if $o(x)$ becomes $o_0(x) = \exp(i2\pi\phi x \tan \delta)$ if $|x| \leq \frac{1}{2}Na$ and $o_0(x) = 0$ elsewhere. Thus with $\nu_c = 0$; $U_0(\nu) = K\psi Na\, [\sin \pi Na\, (\phi \tan \delta - \nu)]/[\pi Na\, (\phi \tan \delta - \nu)]$. The zero order is in the interval $Na\, |\phi \tan \delta - \nu| \leq 1$. For large N this interval is narrow and $(\phi \tan \delta - \nu) \approx 0$ so that $\alpha \approx 2\delta$. Thus ψ (provided δ is not too large) and ϕ can be considered constant; indeed $\psi \approx \cos \delta$ and $\phi \approx (1 + \cos 2\delta)/\lambda$. Integrating over α with λ fixed we get $\Im_0 = 2K^2 Na \cos^2 \delta\, Si(2\pi)/\pi$ where $Si(x) = \int_0 (\sin \zeta/\zeta) d\zeta$.

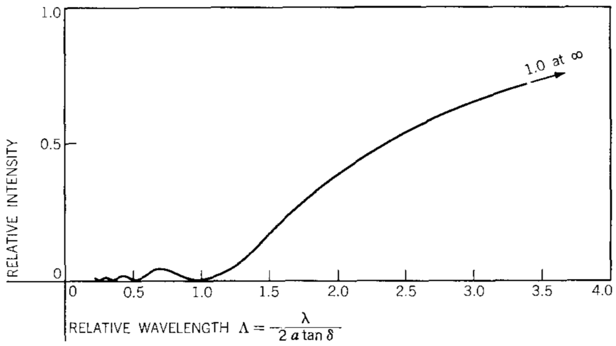

Figure 4 Relative spectral content of the zero order as a function of relative wavelength. Zeros appear at $\Lambda = 1/n$ ($n = 1, 2, 3, \cdots$); only four are shown.

Intensity distribution in the non-zero orders

From Eq. (4a) for the interference function we can see that the m-th order of λ is centered on $\nu_m = \nu_{cm} + m/d$ or $\alpha_m = \sin^{-1}[\sin \alpha_{cm}(\lambda) + (m\lambda/d)]$, where $\alpha_{cm}(\lambda)$ is the angular position of the source. For an infinite grating (or, to good approximation, for a *long* grating) the interference function is simply the comb function ($\sum_{m=-\infty}^{\infty} \delta[\nu - \nu_c - (m/d)]$, where δ is the Dirac delta), so that the m-th order of λ is a discrete line at α_m whose intensity is proportional to

$$\mathfrak{F}_m(\lambda) = [(\psi_m \sin \xi_m)/\xi_m]^2, \qquad (8)$$

where ψ_m and ξ_m are as given by Eqs. (3b) and (4c), respectively, with $\alpha = \alpha_m$ and $\alpha_c = \alpha_{cm}$.

The function $\mathfrak{F}_m$ is plotted in Figs. 5 and 6 for, respectively, the spectrograph configuration (in which light is incident along the normal to the grating and wavelength selection is accomplished by varying the direction of observation) and the Littrow configuration (in which light is returned along the direction whence it came and wavelength selection is accomplished by rotating the grating) for $m = 1, 2, 3$ and $\delta = 15°, 30°$, as a function of the relative wavelength $\Lambda_1 = m\lambda/m_b\lambda_b$ in a grating blazed to the m_b order of the wavelength λ_b. The aspect ratio e is so chosen as to make the adjacent facets ($\overline{AB}$ and $\overline{BC}$ in Fig. 3) perpendicular (which is approximately the case for plane gratings).

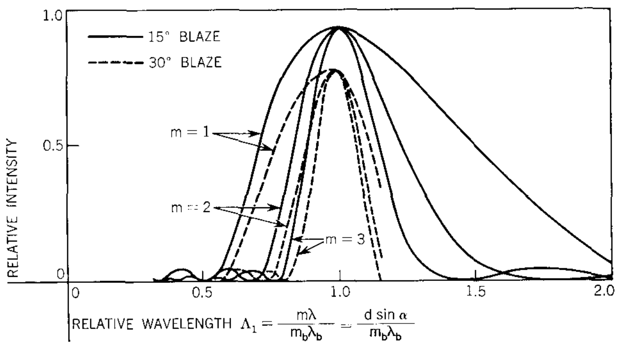

Figure 5 Relative intensity in the first, second, and third orders as a function of relative wavelength, for the 'spectrograph' configuration. (The failure to obtain unity at the maxima is explained on page 116.)

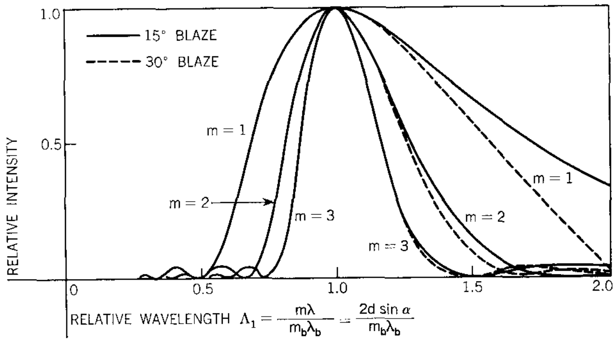

Figure 6 Relative intensity in the first, second, and third orders as a function of relative wavelength, for the Littrow mount configuration.

Figure 7 Relative intensity in the first, second, and third orders as a function of relative wavelength, for the spectrograph configuration, according to linear theory.

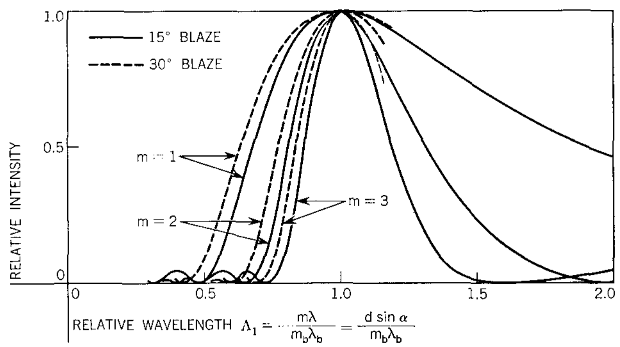

Figure 8 Relative intensity in the first, second, and third orders as a function of relative wavelength, for the Littrow mount configuration, according to linear theory.

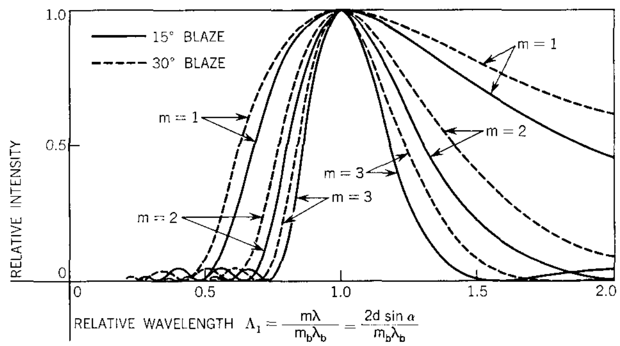

Comparison with linear theory

In the foregoing development, ϕ and ψ are kept as functions of the spatial frequencies ν and ν_c (or of α and α_c). The resultant diffraction pattern $U(\nu)$ differs from $O(\nu)$, the Fourier transform of $o(x)$; the diffraction and object domains are thus not canonically conjugate. Furthermore, ϕ and ψ are not functions of the difference $\nu - \nu_c$ and thus the system is not space invariant (or isoplanatic). These two non-linear effects are important if large values of α and α_c are of interest. In the linear theory we assume that both ϕ and ψ are independent of ν and ν_c. This assumption is valid only over a limited range of α and α_c (given δ). The usual assumption is $\phi = 2/\lambda$ and $\psi = 1$. However, since in a blazed grating the region of observation is in the neighborhood of the blaze wave length, it is more reasonable to chose $\phi = (\cos \alpha_b + \cos \alpha_{cb})/\lambda$ and $\psi = \frac{1}{2}[\cos(\alpha_{cb} + \delta) + \cos(\alpha_b - \delta)]$, i.e., to assume that ϕ and ψ do not vary from the values which they assume when the blaze wave length is observed at α_b when the direction of incidence is α_{cb}. The validity of these assumptions as they affect $\mathfrak{F}_m$ will now be examined.

In the spectrograph configuration, with $\delta = 15°$ in a grating whose facets are perpendicular, ψ varies between 0.90 and 0.98 over the range of $\Lambda_1 = m\lambda/m_b\lambda_b$ between 0.1 and 1.5; with $\delta = 30°$, ψ varies between 0.85 and 0.93 over the range of $0.1 < \Lambda_1 < 1.0$. Thus, in the latter case, the assumption that ψ is constant may lead to a 20% error in $\mathfrak{F}_m$ while the assumption $\psi = 1$ may lead to errors as great as 28% for some wavelengths. In the Littrow configuration with $\delta = 15°$, ψ varies between 0.95 and 1.00 in the range $0.1 < \Lambda_1 < 2.0$; while with $\delta = 30°$, ψ varies between 0.89 and 1.0 in the range $0.1 < \Lambda_1 < 1.7$. Thus, to assume, $\psi = 1$ in the latter case could lead to errors as great as 20% at some wavelengths.

To observe the combined effects of the usual linearizations, consider Figs. 7 and 8 where $(\sin \xi_m/\xi_m)^2$, with $\xi_m = \pi m (\Lambda_1^{-1} - 1) \cos^2 \delta$, is plotted for the spectrograph and Littrow configurations, respectively, with $m = 1, 2, 3$, and $\delta = 15°$ and $30°$. These curves correspond to those in Figs. 5 and 6. As can be seen, the linear theory leads to very considerable errors outside relatively narrow regions in the neighborhood of $\Lambda_1 = 1$, or $\lambda = m_b\lambda_b/m$. *Here, the higher the orders, the narrower the region of validity of the linear theory. Furthermore, according to linear theory, high efficiencies occur over wider regions of wavelength than is actually the case; as a matter of fact, linear theory predicts that the width of these regions increases with blaze angle whereas the opposite is true.* It is clear then, that the rather simple expressions that arise from the linear theory must be used with caution; as would be expected, these expressions provide good approximations only when the blaze angle and the angles of incidence and diffraction are small. For a detailed investigation of the diffraction patterns in the various orders, we shall therefore concern ourselves only with the more general non-linear theory.

Envelope function

The intensity distribution in any order, Eq. (8), is proportional to the square of the envelope function, Eq. (4b). This function depends on the single parameter ξ. *It is of interest to note that ξ represents half the phase difference between the two edges of a single diffracting facet* (A and B in Fig. 3) for light arriving at an angle of incidence α_c measured from the grating normal and diffracted at an angle α to this normal. This property (usually cited for the case of a single slit or for a series of slits[7]) is easily verified, even for blazed gratings, if Eq. (4c) is rewritten as

$$\xi_r = (\pi a/\lambda \cos \delta)[\sin (\alpha_c + \delta) - \sin (\alpha - \delta)] \quad \text{(9a)}$$

(reflecting grating);

$$\xi_t = (\pi a/\lambda \cos \delta)[N_c \sin (\alpha_c + \delta) - \sin (\alpha + \delta)] \quad \text{(9b)}$$

(transmitting grating).

From Figs. 9a-b, it can be seen that

$$\xi_r = \pi(\overline{AD} - \overline{BE})/\lambda; \qquad \xi_t = \pi(N_c\overline{AD} - \overline{BE})/\lambda.$$

Indeed, ξ is then half the phase difference between opposite edges of a single diffracting facet.

In the spectrograph configuration the grating is fixed, and incident light is parallel to the grating normal ($\alpha_c = 0$), so that the parameter ξ is simply

$$\xi_r = (\pi a/\lambda \cos \delta)[\sin \delta - \sin (\alpha - \delta)] \quad \text{(10a)}$$

(spectrograph).

In a monochrometer with an ideal Littrow mount the

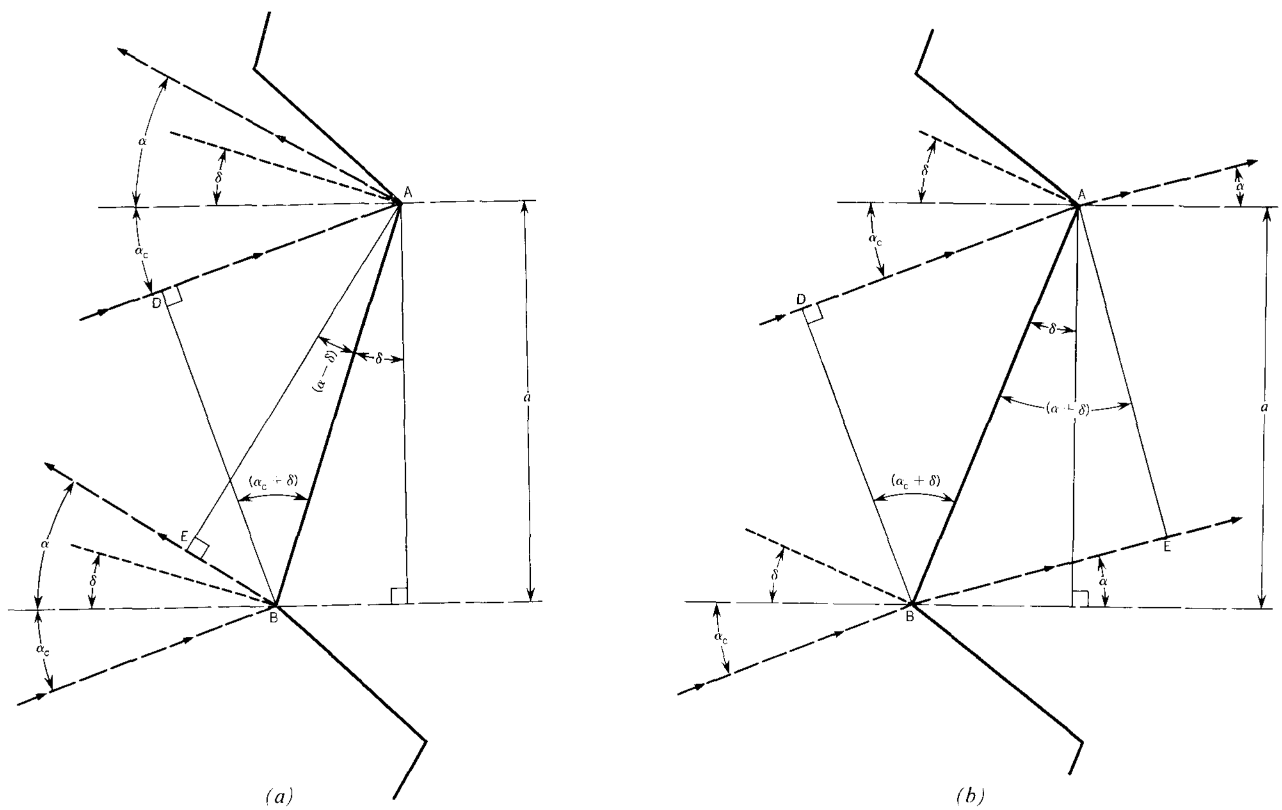

Figure 9 Schematic for the phase relation between incident and diffracted light at the ends of a single facet: (a) reflection grating; (b) transmission grating.

light is returned along the directions whence it came ($\alpha = -\alpha_c$)* and wavelengths are selected by rotation of the grating. Here the parameter ξ is

$$\xi_r = (2\pi a/\lambda \cos \delta) \sin (\delta - \alpha) \quad \text{(Littrow)}. \tag{10b}$$

As can be seen from Figs. 5 and 6 the envelope function is such as to have its maximum value for all orders at the same physical position $\Lambda_1 = 1$, i.e., at $\sin \alpha = m_b\lambda_b/d$. Thus, for example, the wavelength $\lambda_m = m_b\lambda_b/m$ ($m = 1, 2, \cdots$) will overlap the blaze wavelength. This is not serious when gratings are blazed to the first order in the visible range, since the shorter wavelength will either be absent from the source or be absorbed by the optical elements. However, in gratings blazed to a high order (say $m_b > 10$), this can be a serious shortcoming requiring narrow band filters between the source and the grating to eliminate light from orders in the vicinity of m_b.

Blaze angle

The blaze angle is chosen in such a way as to maximize the relative transmission of a particular wavelength λ_b in a particular order m_b, by causing the peak of the envelope function and the desired maximum of the interference function to coincide. As we can see from Eqs. (4b, c), the envelope function attains its maximum value when $\xi = 0$ and is thus centered on $\nu = \nu_c + \phi \tan \delta$. (This is, of course, as would be expected, since the incident plane wave, described by $\exp (2\pi i\nu_c x)$, can be considered as a carrier of spatial frequency ν_c which is frequency-modulated by an object $o(x)$ whose point frequency[14] is $\phi \tan \delta$). We wish this peak to coincide with the m_bth principal maximum of the interference function (which occurs at $\nu = \nu_c + (m_b/d)$ or at $\sin \alpha = \sin \alpha_c + (m_b\lambda_b/d)$, as can be seen from Eq. 4a). Thus, from the above development we see that for a reflecting grating

$$\tan \delta_r = \frac{m_b\lambda_b}{d(\cos \alpha_b + \cos \alpha_{cb})} = \frac{\sin \alpha_b - \sin \alpha_{cb}}{\cos \alpha_b + \cos \alpha_{cb}}, \tag{11a}$$

and for a transmitting grating

$$\tan \delta_t = \frac{m_b\lambda_b}{d(N_c \cos \alpha_{cb} - \cos \alpha_b)} = -\frac{\sin \alpha_b - N_c \sin \alpha_{cb}}{\cos \alpha_b - N_c \cos \alpha_{cb}}, \tag{11b}$$

where α_b and α_{cb} are, respectively, the directions of observation and of incidence (measured from the grating normal) when the grating is in a configuration leading to the observation of the m_b order of λ_b.

Equations (11a) and (11b) can be rewritten as

$$\sin (\alpha_b - \delta_r) = \sin (\alpha_{cb} + \delta_r), \tag{12a}$$

$$\sin (\alpha_b + \delta_t) = N_c \sin (\alpha_{cb} + \delta_t), \tag{12b}$$

and thus the blaze wavelength will be observed at a position defined by α_b such that in the case of a reflecting grating the angle of incidence is equal to the angle of reflection, both angles being measured with respect to the normal to the facet. The diffracting facets can thus be considered as mirrors tilted so as to cause specular reflection in the direction where interference causes the desired principal maximum. In a transmitting grating the blaze wavelength appears in a position for which Snell's law is satisfied. It is interesting to note that Eqs. (12a-b) define the condition under which ξ_r and ξ_t *are zero for all* λ (see Eqs. (9a-b)). Thus the peak of the envelope function for all λ occurs at the position defined by geometric optics. However, only the blaze wavelength and certain other wavelengths, namely $\lambda_m = m_b\lambda_b/m$, with ($m = 1, 2, \cdots$), appear in this position, since only for these wavelengths does a principal maximum of the interference function coincide with the peak of the envelope function.

In a spectrograph $\alpha_{cb} = 0$ and α_b is the position of the m_b order of λ_b defined by $\sin \alpha_b = m_b\lambda_b/d$. Thus from Eq. (11a),

$$\delta_r = \tfrac{1}{2}\alpha_b = \tfrac{1}{2} \sin^{-1} (m_b\lambda_b/d) \quad \text{(spectrograph)}. \tag{13a}$$

Clearly, the blaze wavelength appears at a diffracted angle (measured from the grating normal), which is double the blaze angle.

In a Littrow configuration $\alpha_{cb} = -\alpha_b$ so that from 11a

$$\delta_r = \alpha_b = \sin^{-1} (m_b\lambda_b/2d) \quad \text{(Littrow)}. \tag{13b}$$

and the blaze wavelength appears at an angle equal to the blaze angle as measured from the grating normal.

Aspect ratio

The aspect ratio, $e = a/d$, has appeared in the foregoing discussion. It would be desirable to make this factor unity, since then the minor groove facets contribute very little to the diffraction pattern; this, however, is impossible. In the case of non-blazed grating, i.e., with the blaze angle zero, $e = 1$ means that the diffraction grating is a mirror. It is interesting, of course, to consider what happens when this occurs. We then have specular reflection from a mirror (of a dimension many times larger than that of the wavelength) again described by $(\sin \xi/\xi)^2$. Here, however, this term is very nearly zero in every direction other than that defined by the law of reflection.

In the case where δ is unequal to zero, it is clear that if $e = 1$ then shadowing will affect the spectral efficiency

* It will be noted that by defining α and α_c as in Figs. 2a, b we employ a sign convention which differs from the usual one; the positive direction for diffracted light is on the opposite side of the grating normal from that for the incident light.

in all the higher orders for a large range of λ. How large e can be in practice depends to a large degree on the accuracy allowed by the diamond point of the ruling tool, the mechanics of the ruling engine, etc. For our purposes, however, we shall calculate a useful *maximum* value for this parameter.

Let $\alpha_{\max}$ be the maximum angle of observation associated with a principle maximum of the maximum wavelength involved in the order of interest. The maximum value of e occurs when the minor facets lie in this direction. If these facets were oriented differently, either e would become smaller, or a shadowing effect would occur for some of the incident light; diffraction effects (Huygens wavelets) will arise around this shadowing lip, and will contribute to the over-all diffraction pattern. Under the above conditions the value of e becomes, Fig. 10,

$$e = a[a + (d - a)]^{-1} = (1 + \tan\delta \cdot \tan\alpha_{\max})^{-1}. \quad (14)$$

This expression defines a useful maximum aspect ratio given a desired $\alpha_{\max}$. Furthermore, given e, Eq. (14) defines $\alpha_{\max}$, the limiting direction for which no shadowing occurs. In the special case of a grating whose grooves consist of perpendicular facets $\alpha_{\max} = \delta$ and $e = \cos^2\delta$.

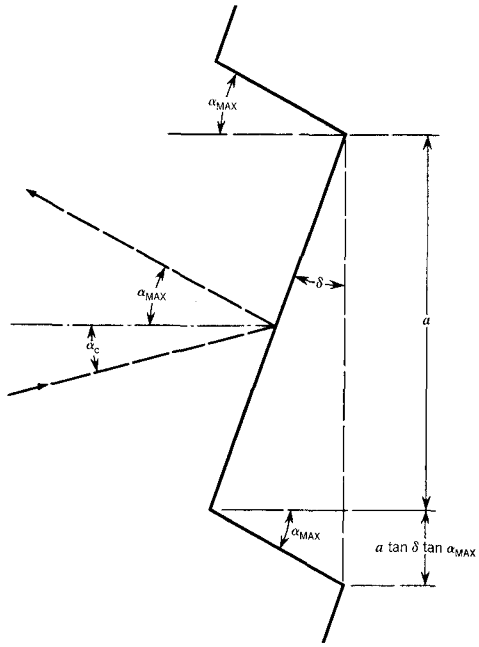

Figure 10 Geometry for determination of the useful maximum aspect ratio.

Observations

1) Since the various wavelengths are not uniformly distributed in the zero order, Fig. 4, this order does not appear "white". As we have observed, the wavelengths $\lambda_n = (2a\tan\delta)/n$, with $n = 1, 2, \cdots$, are missing from this order.

In the spectrograph and Littrow configurations, the variable $\Lambda = \lambda/(2a\tan\delta)$ appearing in Eq. (7) assumes the values, see Eqs. (13a-b),

$$\Lambda = (\lambda/em_b\lambda_b)\cos^2\delta \text{ (spectrograph)} \quad (15a)$$

$$\Lambda = (\lambda/em_b\lambda_b)\cos\delta \text{ (Littrow)} \quad (15b)$$

The blaze wavelength λ_b will thus be missing if, for instance, $e = e_s = \cos^2\delta$ in the spectrograph configuration, or $e = e_L = \cos\delta$ in the Littrow configuration.

If $\lambda < 2a\tan\delta$ (and thus if $\lambda < \lambda_b$ in gratings blazed to the first order and having $e_s \leq \cos^2\delta$, or $e_L \leq \cos\delta$) then $\mathfrak{I}_\infty(\lambda) < .05\ \mathfrak{I}_\infty(\infty)$. *The shorter wavelengths are almost entirely diffracted into the higher orders while the very long wavelengths are unaffected by the grating;* the latter appear in the zero order having been reflected back along the grating normal whence they came.

2) In general, the higher orders do not have a uniform transmission with respect to wavelength. As a matter of fact, only in an unblazed grating—where $\xi_m = -\pi em$ is independent of λ and where $\psi_m = \frac{1}{2}(\cos\alpha_{cm} + \cos\alpha_m)$ is a slowly varying function of λ—is the intensity distribution nearly constant with wavelength. A special case of interest is the plane mirror ($e = 1$) for which $\mathfrak{F}_m(\lambda) = 0$ for all λ in all the non-zero orders, which is as would be expected.

As the blaze angle is increased from zero, $\mathfrak{F}_m$ becomes more dependent on λ. As we have seen above $(\sin\xi_m/\xi_m)^2$ attains its peak for $\lambda_m = m_b\lambda_b/m$, with $m = 1, 2, \cdots$. Furthermore, $\mathfrak{F}_m$ has zero's when $\xi_m = k\pi$.

3) *One property of blazed gratings is that all orders have zeros at those geometric positions where the first order has zeros;* i.e., there are 'dark' lines into which no light is transmitted in any order. This is easily verified when we examine Eq. (9a), fixing the angles of observation and of the source (α and α_c respectively) at their values for which the first order has zeros, namely $\alpha_1^{(k)}$ and $\alpha_{c1}^{(k)}$ associated with $\lambda^{(k)}$ for which $\xi_1^{(k)} = k\pi$ ($k = 1, 2, \cdots$) and thus, $\mathfrak{F}_1[\lambda^{(k)}] = 0$. Then in the mth order at these positions—i.e., at $\alpha_m^{(\ell)} = \alpha_1^{(k)}$ and $\alpha_{cm}^{(\ell)} = \alpha_{c1}^{(k)}$—we observe $\lambda^{(\ell)} = \lambda^{(k)}/m$. But for these wavelengths (see Eq. (9a)) $\xi_m^{(\ell)} = m\xi_1^{(k)} = \ell\pi$ where $\ell = mk$ is an integer, and thus $\mathfrak{F}_m[\lambda^{(\ell)}] = 0$. We see then that at position $\alpha_1^{(k)}$ and $\alpha_{c1}^{(k)}$ all orders have zeros, as was to be shown.

4) It is convenient to use Λ_1 as the independent variable (even though it is a function of m and thus leads to different scales in the different orders) since the relative transmission is then directly related to the actual position where the

diffracted light appears. This follows from the fact that $\Lambda_1 = m\lambda/m_b\lambda_b = \kappa \sin \alpha$, where α defines the position at which the various wavelengths λ are observed with $\kappa = \kappa_s = d/m_b\lambda_b$ in the spectrograph configuration, and $\kappa = \kappa_L = 2d/m_b\lambda_b$ in the Littrow configuration. *Thus the abscissa in Figs. 5 and 6 (and Figs. 7 and 8 as well) is proportional to sin α for all m,* and we see the dark lines at the zero's of the relative transmission in the first order.

5) Each order has a different relative transmission since the dependence of $\mathfrak{T}_m$ on m arises from the dependence on m of both Λ_1 and ξ_m. The latter is given by

$$\xi_m = \tfrac{1}{2}\pi m[\Lambda_1^{-1}(1 + \sqrt{1 - \Lambda_1^2 \sin^2 2\delta}) - \cos 2\delta - 1] \quad \text{(spectrograph);} \quad (16a)$$

$$\xi_m = \pi m(\Lambda_1^{-1}\sqrt{1 - \Lambda_1^2 \sin^2 \delta} - \cos \delta) \cos \delta \quad \text{(Littrow).} \quad (16b)$$

6) The contribution of ψ to the relative transmission $\mathfrak{T}_m$ can be seen from the expressions

$$\psi_s = \frac{[\Lambda_1 \sin^2 2\delta + (1+\sqrt{1-\Lambda_1^2 \sin^2 2\delta})(1+\cos 2\delta)]}{2\sqrt{2}\,\sqrt{1+\cos 2\delta}} \quad \text{(spectrograph);} \quad (17a)$$

$$\psi_L = \Lambda_1 \sin^2 \delta + \cos \delta \sqrt{1 - \Lambda_1^2 \sin^2 \delta} \quad \text{(Littrow).} \quad (17b)$$

In the latter case $\psi_L(\lambda_b) = 1$ for all δ. This is not true in the spectrograph configuration where at the blaze wavelength ψ_s is a function of δ. It is this factor which causes the relative transmission in the spectrograph to be less than 1.0 at the blaze wavelength, Fig. 5.

7) It should be noted that *longer wavelengths can be observed with the Littrow than with the spectrograph configuration.* This is due to the fact that in any order the maximum observable wavelength must be such that the quantity $\lambda m/d$ is 1 in the spectrograph configuration, but 2 in the Littrow configuration. These wavelengths correspond to $\alpha = \pi/2$ and are thus in the region where shadowing and multiple diffraction effects become important.

Contribution of the minor facets

To include the contribution of the minor facets we must replace $U(x)$ by $U_1 = U + U'$ where $U'(x)$ can be obtained from $U(x)$ by replacing K, ψ, and $o(x)$ in Eq. (3) by K', ψ', and $o'(x)$, respectively. The latter are simply ψ and $o(x)$ as given in Eqs. (3a–c), with δ replaced by $-\delta'$, and k by k', where δ' is the blaze angle of the minor facets and $k' = k + \frac{1}{2}$.

The intensity distribution is then

$$U_1 U_1^* = \left| I(\nu)[K\psi E e^{-i2\pi(\nu-\nu_c)kd} + K'\psi' E' e^{-i2\pi(\nu-\nu_c)k'd}]\right|^2, \quad (18)$$

where $I(\nu)$ is the interference function as given in Eq. (4a) and E' is the envelope function associated with the minor facets and having the form of E given in Eq. (4b) but with a replaced by $a' = d - a$ and ξ replaced by ξ', obtained from ξ as given in Eq. (4c) by replacing a and δ by a' and $-\delta'$, respectively.

The peak of the envelope function E' associated with the minor facets will be at $\xi' = 0$. This is on the other side of the normal from the peak in E. The two envelope functions interfere, however, but the contribution of one to the amplitude in the vicinity of the peak of the other is quite small.

It should be noted that, subject to minor revision, the foregoing observations apply to the present case as well. Thus for example, the wavelengths missing from the zero order of E' are the same as those missing from E since $n\lambda_n' = 2a' \tan \delta' = 2a \tan \delta = n\lambda_n = 2h$ where h is the groove depth. Also, to the extent that the interference of E and E' can be neglected (each contributes little to the distribution on the opposite side of the grating normal from that in which it attains its peak) the dark lines at those locations where the first order is zero remain dark. However, for certain values of the ratio α/α' some of the zero's of the first order of E' will overlap those of E. Thus for such a grating, dark lines will indeed exist. All such ratios can be obtained from the constraint that $\xi' = m'\pi$, for some integer m' will fall at the same geometric location as $\xi = m\pi$ for some integer m.

Conclusions

We have shown that the linear theory (which neglects the dependence of the phase deviation and obliquity factor on spatial frequency) is valid only over a limited range of angles of incidence and diffraction. It provides a general picture of the relative transmission of a grating in any order but leads to gross quantitative errors.

Several interesting properties of the relative transmission of diffraction gratings in the various orders have been examined on the basis of a scalar non-linear theory. It has been shown that dark lines exist at the zero's of the first order and that certain wavelengths are essentially missing in the zero order. We have also given a detailed description of the diffraction fields of a blazed grating in the spectrograph and Littrow configurations.

Acknowledgments

The authors are indebted to Dr. R. V. Pole and Mr. C. Smoyer for many fruitful discussions on the subject of blazed gratings, to Professor G. W. Stroke for his useful suggestions, and to Dr. H. Freitag for his help in the calculations incorporated herein.

References

1. R. W. Wood, "On a Remarkable Case of Uneven Distribution of Light in a Diffraction Grating Spectrum," *Phil. Mag.* **4**, 396–402 (1902).
2. R. W. Wood, "Diffraction Gratings with Controlled Groove Form and Abnormal Distribution of Intensity," *Phil. Mag.* **23**, 310–317 (1912).
3. R. W. Wood, *Physical Optics*, MacMillan, New York, 1934, 3rd ed., (see p. 264).
4. Lord Rayleigh, "On the Dynamical Theory of Gratings," *Proc. Roy. Soc.* (London) **A79**, 399–416 (1907).
5. R. P. Madden and J. Strong, "Diffraction Gratings," Appendix P in J. Strong, *Concepts of Classical Optics*, W. H. Freeman and Co., San Francisco, 1958.
6. E. S. Barrekette and H. Freitag, "Diffraction by a Finite Sinusoidal Phase Grating," *IBM Journal* **7**, 345 (1963).
7. F. A. Jenkins and H. E. White, *Fundamentals of Optics*, McGraw-Hill Book Co., Inc., New York, 1950, 2nd ed., (see p. 323).
8. A. Maréchal and G. W. Stroke, "Sur l'Origine des Effets de Polarisation et de Diffraction dans les Réseaux Optiques", *Compt. Rend.* **249**, 2042 (1959).
9. G. W. Stroke, "Etude Théorique et Experimentale de deux aspects de la diffraction dans les réseaux optiques: L'évolution des defauts dans les figures de diffraction et l'Origine Electromagnetique de la Répartition entre les Ordres," *Rev. Opt.* **39**, 291 (1960).
10. P. Bousquet, "Diffraction des Ondes Electromagnétiques par un Réseau à Facettes Planes," *Compt. Rend.* **256**, 3422 (1963).
11. P. Bousquet, "Diffraction des Ondes Electromagnétiques par un Réseau à Profil Triangulaire," *Compt. Rend.* **257**, 80 (1963).
12. G. W. Stroke, "Diffraction Gratings," in *Handbuch der Physik*, Vol. 29, edited by S. Flügge, Springer-Verlag, Berlin (to be published).
13. M. Born and E. Wolf, *Principles of Optics*, Pergamon Press, New York, 1959.
14. R. V. Pole, "On Spatial Frequencies and Optical Systems with Partially Coherent Illumination," IBM Report RC-772, August, 1962.
15. R. V. Pole, "Spatial Phase Modulation and Remodulation," appearing in E. L. O'Neill, *Communications and Information Theory Aspects of Modern Optics*, General Electric Co., Electronics Laboratory, Syracuse, August, 1962.
16. R. S. Longhurst, *Geometrical and Physical Optics*, Longmans, Green and Co., Ltd., London, 1957 (see p. 230).

Received October 29, 1964.